Comparison of Ribonucleic Acid Homopolymer Ionization Energies and Charge Injection Barriers

J. Magulick,† M. M. Beerbom, and R. Schlaf*

Department of Electrical Engineering, University of South Florida, Tampa, Florida 33620

Received: April 10, 2006; In Final Form: May 24, 2006

Thin films of guanosine and uridine ribonucleic acid (RNA) homopolymers (poly rG, poly rU) were grown in high vacuum in several steps on highly oriented pyrolytic graphite (HOPG) using electrospray deposition. Between deposition steps, the sample surface was characterized with X-ray and ultraviolet photoemission spectroscopy (XPS, UPS). The resulting spectra series allowed the determination of the orbital alignment at the HOPG interface, as well as the ionization energies of the homopolymer thin films. Comparison with earlier results on cytidine and adenosine RNA homopolymers (poly rC, poly rA) indicates significant ionization energy and charge injection barrier differences between purines and pyrimidines.

Introduction

The determination of the ionization energy of nucleic acid related molecules has now been a focus of theoretical[1−4] and experimental research for several decades. Most of the published experimental results were either obtained through gas-phase photoemission spectroscopy[4] or ion current threshold measurements[5] on nucleobases, mononucleosides, and mononucleotides. Recently, electrospray injection enabled the investigation of trinucleotides in the gas phase.[6]

In contrast to these earlier experiments, the experiments presented here focus on the investigation of nucleotide homopolymers having chain lengths of hundreds of monomers. The experiments were performed using photoemission spectroscopy on thin films to measure the ionization energy of nucleotide homopolymers, and to investigate charge injection barriers between these nucleotide polymers and an inorganic material, highly oriented pyrolytic graphite (HOPG). HOPG was chosen for these initial (experiments on other nucleotide contacts are currently underway) investigations for its chemical inertness and its weak valence band emissions. This allowed the measurement of the electronic structure of nucleotide polymers without significant interference from the substrate, enabling the measurement of the density of states and ionization energy of ribonucleic acid (RNA) in its solid state.

The motivation for these experiments, beyond the basic challenge to measure the electronic structure of nucleotide polymers, originates mainly from the need to better understand the contacts between nucleotides in the solid state and inorganic materials such as encountered in conductivity measurements on DNA strands[7−11] or in the self-assembly of nanostructures using specific DNA hybridization.[12,13] In particular, the outcomes of conductivity measurements on single DNA strands, which can range from insulating over semiconducting to metallic, call for a detailed investigation of the orbital alignment at nucleotide/inorganic interfaces. While the experiments described here are not directly relevant to such conductivity measurements, because HOPG is not a commonly used electrode material, the results indicate significant differences between the charge injection barriers relative to the HOPG Fermi level for each of the nucleotide polymers. This suggests that similar differences are likely also to be found at contacts to electrode materials such as Au or Pt, which may partially account for the wide spread of DNA conductivity data.

The purpose of this paper is to describe experimental results on the polyguanosine (poly rG)/HOPG and polyuridine (poly rU)/HOPG interfaces in detail, and to discuss the results in light of previously published investigations of the polyadenosine (poly rA)/HOPG[14] and polycytidine (poly rC)/HOPG[15] interfaces, allowing direct comparison between all four RNA nucleotide interfaces, HOMO electronic structures, and ionization energies.

The technique used for these investigations is based on a methodology established earlier for the characterization of inorganic semiconductor contacts utilizing photoemission spectroscopy in combination with in-vacuum deposition.[16] In particular, one of the contact-forming materials is usually deposited in several steps on top of a substrate of the other material. Before and between deposition steps, the sample surface is characterized with X-ray and ultraviolet photoemission spectroscopy (XPS, UPS) without breaking the vacuum. This requires a deposition setup that is directly integrated with the photoemission chamber as well as an appropriate in-vacuum deposition technique allowing contamination-free thin film growth. Because nucleotide polymers are too heavy and thermally fragile for in-vacuum evaporation, a recently developed electrospray deposition system[17] was utilized, which allowed the direct injection of the RNA homopolymers from solution into high vacuum.

Using this setup, poly rG and poly rU thin films were grown in several steps on in-vacuum-cleaved HOPG crystals without breaking the vacuum. Between deposition steps, the surface was characterized with XPS and UPS. The resulting series of spectra allowed the determination of the orbital line-up of the nucleotide homopolymers relative to the HOPG Fermi level and the determination of their ionization energies. Comparison with the poly rA and poly rC data revealed that the purines have a significantly smaller ionization energy, as well as smaller hole injection barriers, than the pyrimidines. This is in qualitative agreement with earlier published gas-phase photoemission data and theoretical calculations.

* Corresponding author. E-mail: schlaf@eng.usf.edu. Fax: 813-974-5250.

† Undergraduate research assistant.

10.1021/jp062231j CCC: $33.50
Published on Web 07/26/2006

Experimental Section

Experiments were performed in an ultrahigh vacuum (UHV) system manufactured by SPECS GmbH (Berlin, Germany), which consists of a fast-entry load lock, two preparation chambers, and an analysis chamber equipped with XPS and UPS. The system operates at a base pressure of approximately 2×10^{-10} mbar. A home-built electrospray injection system was flanged to one of the preparation chambers via two differential pumping stages operating at 0.1 mbar and 3×10^{-4} mbar (for more details on the system, see ref 17). An in situ transfer system allowed the transfer of samples between preparation and analysis chambers without breaking the vacuum. The deposition of poly rU (Midland Reagent Company, Inc.; 200−800 nucleotides length; >95% purity) and poly rG (Sigma Aldrich Co., average weight 450 000 Da, corresponding to a chain length of 1238 nucleotides, purity >98%) was accomplished by injecting 1 mg/mL aqueous solution through a 100 μm stainless steel capillary into the electrospray system intake (1 mm diameter orifice) at 4 mL/h injection rate. Contamination from the ambient was reduced to insignificant levels in the UHV system by flowing nitrogen gas at slight overpressure relative to atmosphere through the capillary enclosure during deposition. The pressure rose to approximately 10^{-5} mbar in the preparation chamber during deposition.

To obtain a pure, clean surface for polynucleotide deposition, HOPG crystals (Mikromasch USA, "ZYA" quality) were cleaved in situ. Cleavage was accomplished by attaching a metal foil to the top of the HOPG crystal via silver epoxy. A manipulator arm in the UHV system was then used to remove the metal foil along with the top layers of substrate, creating a pristine graphite surface. Multistep deposition series were carried out for the determination of the electronic structure of the deposited polynucleotide layers and the interfaces to HOPG. After cleavage and after each deposition step, the sample surfaces were characterized by nonmonochromatized XPS and UPS. Low-intensity XPS (LIXPS, see ref 14 for details on this procedure) work function measurements were performed after all deposition steps to quantify the magnitude of sample charging artifacts in UPS measurements. All measurements on the multistep prepared samples were performed using a SPECS XR 50 X-ray source (Mg Kα; $h\nu = 1253.6$ eV) and a SPECS UVS 10/35 ultraviolet source (HeI; $h\nu = 21.22$ eV). Separate samples of similar nucleotide polymer film thickness such as the final layers prepared during the multistep experiments were prepared for stoichiometry analysis. These measurements were performed using a monochromatized X-ray source (SPECS FOCUS 500 ellipsoidal crystal monochromator; Al Kα ($h\nu = 1486.6$ eV)) to increase the resolution. During all measurements, the spectrometer was calibrated to yield the standard Cu $2p^{3/2}$ line at 932.66 eV and the Cu $3p^{3/2}$ line at 75.13 eV.[18]

Analysis of all photoemission spectra was carried out using Igor Pro (Wavemetrics, Inc.). Cutoff positions were determined by fitting lines to the spectral onset and determination of the intersect with the baseline. To correct for analyzer broadening, a value of 0.1 eV was added to all cutoff positions (estimated from the Fermi edge width (0.2 eV)[19]). The monochromatized XPS spectra were fitted using a procedure outlined in ref 20.

Results

The XP spectra of the O 1s, N 1s, and P 2p emission lines measured during the two multistep deposition series are shown in Figure 1 (top panels: poly rG/HOPG; bottom panels: poly rU/HOPG). The bottom spectra of each of the series correspond to the cleaved HOPG substrate. While N 1s and P 2p regions appear flat in both experiments, a weak emission is apparent at around 532 eV in the O 1s regions. These features are related to emissions from the oxidized substrate holder assembly. As the deposition volume increases, the characteristic features of the oligonucleotides appear.

Considering first the poly rG data, the O 1s region appears to consist of three emission lines. The primary line occurs at about 534.1 eV, while the secondary emission lies at about 532 eV. The third line is only manifested as a weak shoulder on the high binding energy side at approximately 535.7 eV. The N 1s emission feature appears to consist of two lines of approximately equal intensity at about 400.1 and 401.7 eV. The P 2p emissions consist of a single peak at a position at around 134.8 eV. The poly rU data look similar, with the exception that the N 1s peak is much narrower, suggesting only a single emission line located at about 402 eV. The O 1s line again includes three emissions at about 534, 532, and 535.7 eV. The P 2p line is again only composed of a single emission at 134.8 eV.

Figure 2 shows the corresponding UP spectra measured after each deposition step of the two deposition series (poly rG (top), poly rU (bottom)). The full spectra are shown in the center. The spectra include three main regions of interest: (1) HOPG valence bands and nucleotide HOMO emissions between 0 eV and approximately 9 eV, (2) a peak at about 13.6 eV corresponding to electrons that are inelastically scattered into a high density of states region of the HOPG conduction band, (3) secondary edge (high binding energy cutoff of the spectra). This region is shown again normalized in the graphs on the left for better comparison. Generally, as the layer thickness increases, the HOMO emissions from the polynucleotides appear between approximately 2−9 eV, while the HOPG related features are attenuated. In both experiments, the secondary edge remains unchanged during the first deposition steps and then shifts to higher binding energy. This shift is a result of charging artifacts due to the photoemission process, which was confirmed through additional measurements of the cutoff using low-intensity X-ray photoelectron spectroscopy (LIXPS).[14] In this method, low-intensity X-rays (having an approximately 5 magnitudes lower photon flux compared to that of the UV source used in these experiments) is used to measure the secondary cutoff before and after the UPS measurement. These measurements showed that the secondary edge does not shift at all during the entire experiment when measured with LIXPS (the LIXPS spectra series looks very similar to the one shown in Figure 4 in ref 14), allowing the conclusion that the shifts seen in the UP spectra are entirely charging related, in concordance with earlier measurements on poly rA[14] and poly rC.[15]

Figure 3 shows O 1s, N 1s, C 1s, and P 2p core levels measured with monochromatized X-rays on separate poly rG (left) and poly rU (right) thin films of similar thickness as the final layers of the multistep depositions. The added peaks represent the fitted spectra associated with the various chemical environments encountered by each atomic species in the molecules.

Discussion

A. Stoichiometry and Morphology. From the molecular structures (shown on top in Figure 5), it follows that poly rG contains 7 oxygen, 5 nitrogen, 1 phosphorus, and 10 carbon atoms, while poly rU contains 8 oxygen, 2 nitrogen, 1 phosphorus, and 9 carbon atoms per nucleotide.

Ideally, the total peak areas of the related core level lines should reflect these atomic ratios. Hence, a peak area evaluation of the entire emission features shown in Figure 3 was performed

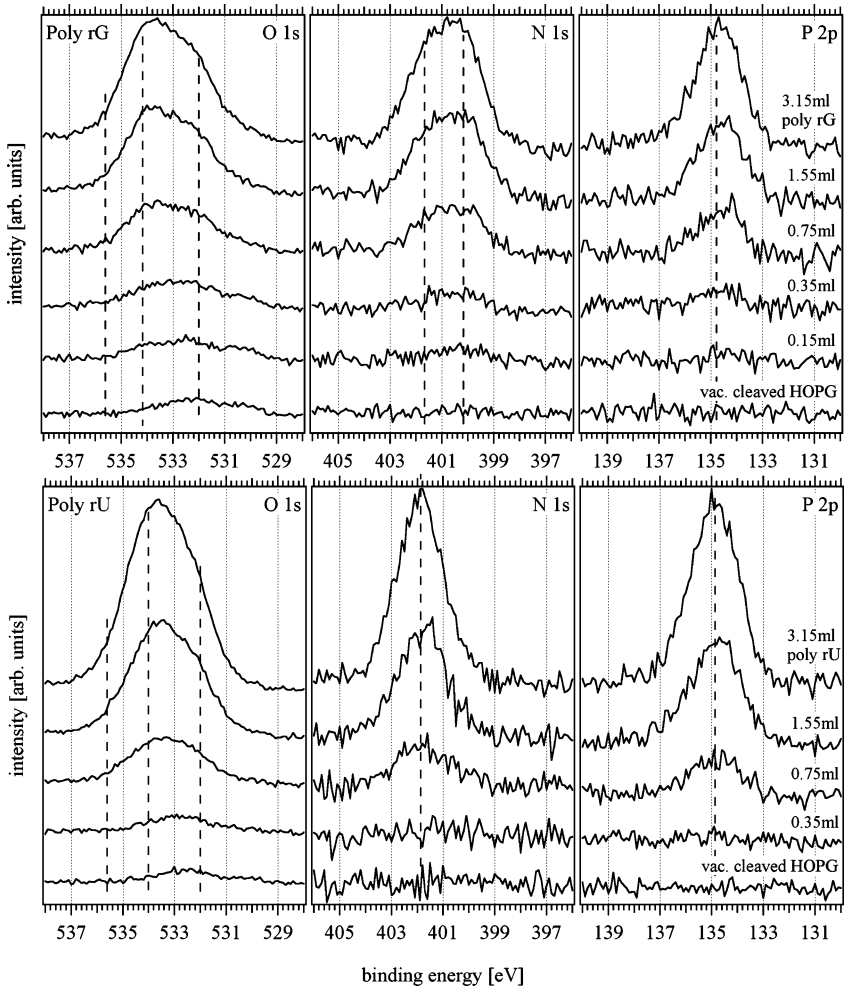

Figure 1. O 1s, N 1s, and P 2p core level XPS spectra measured on cleaved HOPG and after each deposition step. The top graphs correspond to poly rG, while the bottom graphs correspond to poly rU. The parameter is injected oligonucleotide solution volume. Charging artifacts are observed in the final deposition step in the slight shift to a higher binding energy.

to find the total relative intensities between each atomic species using the same procedure described in ref 14. Table 1 lists the assumed ionization cross sections, mean free paths, and transmission factors as well as the calculated relative intensities with respect to phosphorus for each of the two oligonucleotides. The relative intensity ratios obtained for poly rG between P 2p and O 1s (5.76:1) and N 1s (3.54:1) are lower than the theoretically expected values (7:1 for O 1s and 5:1 for N 1s) but fall within experimental uncertainty if no standards are used. The values are in good agreement with results by May et al.,[21] where the area ratios measured on guanidine oligomers were also somewhat lower than the stoichiometric ratios (6.21:1 for O 1s, 4.35:1 for N 1s). The analysis for poly rU is similar in that obtained relative ratios amount to 6.48:1 for O 1s and 1.44:1 for N1 s. Results from May et al.[21] are again similar, with relative ratios of 7.18:1 for O 1s and 1.72:1 for N 1s. The C 1s ratio for poly rG, 10.04:1 agrees well with the theoretical ratio of 10:1, which is probably related to the absence of purely C−C bonded C in poly rG (i.e., the substrate emissions do not interfere significantly with the overlayer emissions, facilitating their analysis). Poly rU, on the other hand, exhibits a too high relative intensity ratio for non-C−C related emissions of 10.51:1 compared to the theoretical ratio of 8:1 for C−O, N−C, N−(C═O)−N, and N−(C═O)−C structures. One can speculate that this may be related to overlap with substrate emissions because poly rU has one C atom in a pure C−C environment.

The next step is the evaluation of the intensities and binding energies of the constituting lines of each spectrum and try to match this information with the chemical environments encountered by each atomic species in both poly rG and poly rU. The O 1s curve fits to the emission lines of poly rG and poly rU are shown in Figure 3A and B (solid lines). The individual peaks correspond to O atoms in different chemical environments. In the case of poly rG, the fitting procedure yielded three O 1s peaks with maxima at 532.2, 533.9, and 535.7 eV, having full widths at half-maximum (fwhm) of 1.81, 1.91, and 1.81 eV, respectively. In poly rG, four of the oxygen atoms are bonded to the ribose sugar or between the ribose and the phosphate, two are single or double bonded to the phosphorus, and one is double bonded to carbons in the nitrogenous base. Hence, oxygen atoms in the phosphate, which appear in a range from 530.5 to 532.5 eV,[22] and double-bonded oxygens in the base, which emit around 532.3 eV,[23] can be assigned to the secondary peak. The small shoulder at 535.7 eV is probably related to coadsorbed water, similar to what was found in previous experiments on poly rC and poly rA/HOPG interfaces.[14,15] The O atoms in C−O−P structures, which yield O 1s peaks at 533.37 eV,[23] and C−O−C structures, which occur in a range from 532.94 to 533.59 eV,[23] are left to be assigned to the more prominent emission at 533.9 eV. Similar O environments can also be found in the poly rU oligomer, where four oxygens are found in the ribose sugar, two are directly bonded to the

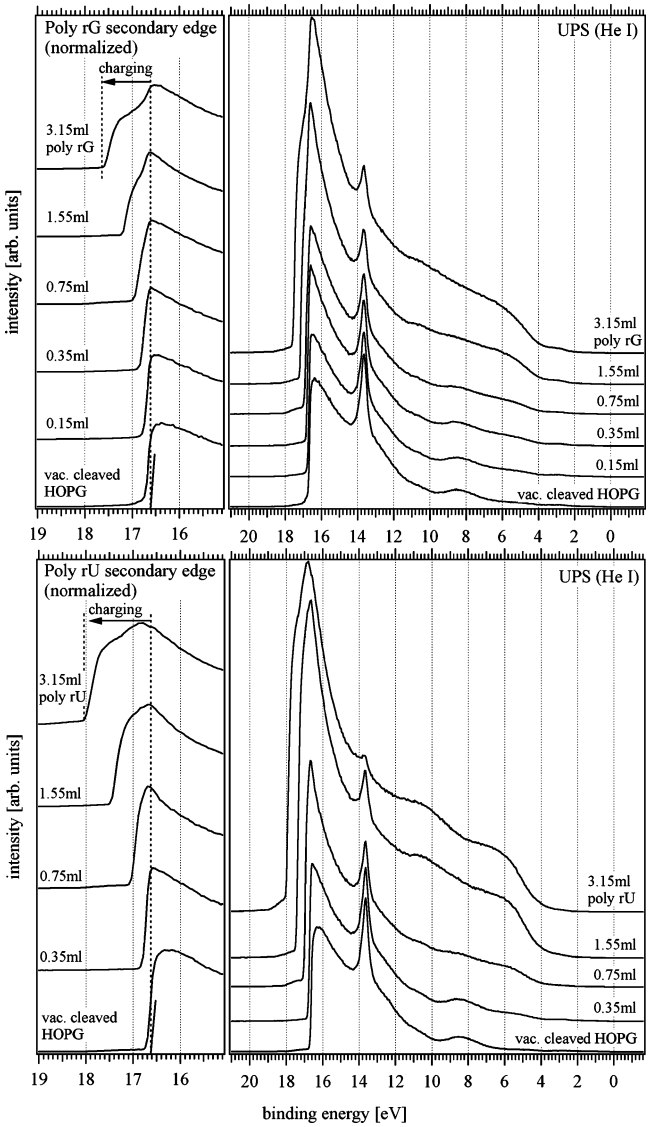

Figure 2. UP spectra corresponding to XPS measurements shown in Figure 1. Top: Poly rG. Bottom: Poly rU. Full spectra are shown on the right. The left graphs show the normalized secondary edge (high binding energy spectral cutoff). The shifts to higher binding energy of the cutoff are related to charging artifacts.

phosphate, and two are double bonded in the base. The performed fit yielded three peaks that have maxima at 532.6, 534.1, and 535.7 eV, while having fwhm of 1.86, 1.96, and 1.62 eV, respectively. Therefore, the same assignments were made with C−O−P and C−O−C structures assigned to the more prominent peak, phosphate and double-bonded oxygens assigned to the secondary peak, and water assigned to the weak high binding energy shoulder. Determination of the intensity ratios between the main and secondary O 1s peaks yielded 1.73:1 for poly rG and 1.52:1 for poly rU. Both of these values disagree with the theoretical values of 1.33:1 for poly rG and 1:1 for poly rU. The discrepancy can be attributed to the curve fitting process. Tautomerization of the nucleotides may also affect these ratios.

Curve fits to the N 1s emissions are shown in Figure 3C and D. The poly rG spectrum was fitted with two lines with maxima at 400.2 and 401.6 eV and fwhm of 1.9 and 1.98 eVrespectively. The structure of poly rG contains four nitrogens in the purine ring and one $-NH_2$ substituent. The peaks may be assigned to conjugated and nonconjugated nitrogen in the purine base, where conjugated nitrogen emits at a lower binding energy at approximately 399.0 eV and nonconjugated emits at around 400.6 eV.[24] Hence, it is possible to tentatively assign the two nonconjugated nitrogens to the higher binding energy line, and the two conjugated nitrogens to the lower binding energy line. Furthermore, it has been shown in measurements on NH_2 ligands[25] that NH_2 related emissions occur at around 400 eV, which would match the low binding energy line. However, the intensity ratio between the main and secondary peak is 1.11:1, not 3:2 as would be expected through the reasoning above. This may again be related to possible tautomerization and fitting errors. When examining the corresponding poly rU N 1s spectrum, the fit for poly rU yielded a single peak with a maximum at 402.0 eV and a fwhm of 1.97 eV, suggesting that the two nitrogens are in similar, not conjugated, chemical environments. This is in good agreement with the structure of poly rU.

Parts E and F of Figure 3 show the curve fits for the corresponding C 1s region. The poly rG C 1s spectrum was fitted with four peaks having maxima at 284.6, 285.4, 287.4, and 288.8 eV and fwhms of 0.65 eV, 1.30, 1.94, and 1.72 eV, respectively. The following peak assignments can be made when comparing to the structure of poly rG: the most prominent peak corresponds to C−C emissions from the HOPG substrate because guanosine does not feature C atoms in pure C environments, i.e., does not contribute significantly to this peak. The peaks at higher binding energy represent carbon bound to oxygen in the ribose sugar and carbon bound to nitrogen in the purine rings. XPS analysis of nucleotides immobilized on gold found binding energies for carbons in the purine and ribose substituents to occur at around 286.5 eV for C−O bonds, and around 286−287 eV for C−N bonds.[21] This range of binding energies makes assignment of each species to specific peaks difficult. The carbonyl in the purine ring can be assigned to the high binding energy peak because N−(C═O)−C structures are found to occur at 288 eV.[21] The poly rU spectrum was fitted using four lines having maxima at 284.6 eV, 286.0, 287.9, and 290.1 eV and fwhms of 0.67, 1.94, 1.90, and 1.99 eV, respectively. Similar peak assignments such as in poly rG may be made for poly rU when examining its structure. The most prominent peak is assigned to C−C emissions from the substrate and the one carbon bound to two other carbons in the pyrimidine ring. Similarly, C−N and C−O bonds in the pyrimidine ring and ribose sugar can be assigned to the intermediate peaks, and the two carbonyls can be assigned to the high binding energy peak, given that N−(C═O)−N structures are known to occur at 289 eV.[21] It should be noted that the binding energies obtained here are consistently about 1 eV higher than the values cited in ref 21. The discrepancy is probably due to differences in instrument calibration, or the formation of interface dipoles between substrates and DNA overlayers in the cited experiments, offsetting the core level positions relative to the substrate Fermi energy.

The P 2p curve fits are shown in Figure 3G and H. These fits were performed using a single 2:1 intensity ratio double representative of p-orbital emissions because there is only one P atom per nucleotide. This analysis yielded the P $2p_{3/2}$ and $2p_{1/2}$ positions in poly rG to be 134.5 and 135.3 eV, and the positions in poly rU to be 134.8 and 135.6 eV, respectively.

The morphology of the interface was analyzed using the attenuation of the conduction band related feature at 13.6 eV in the UP spectra. The outcomes of this evaluation were very similar to what was reported in refs 14, 15. This allows the conclusion that the surface morphology of the poly rU and poly rG thin films was similar to what was seen on the poly rA and poly rC surfaces, indicating that the surface was largely covered by flat thin films with a small surface area covered by three-dimensional deposition artifacts.

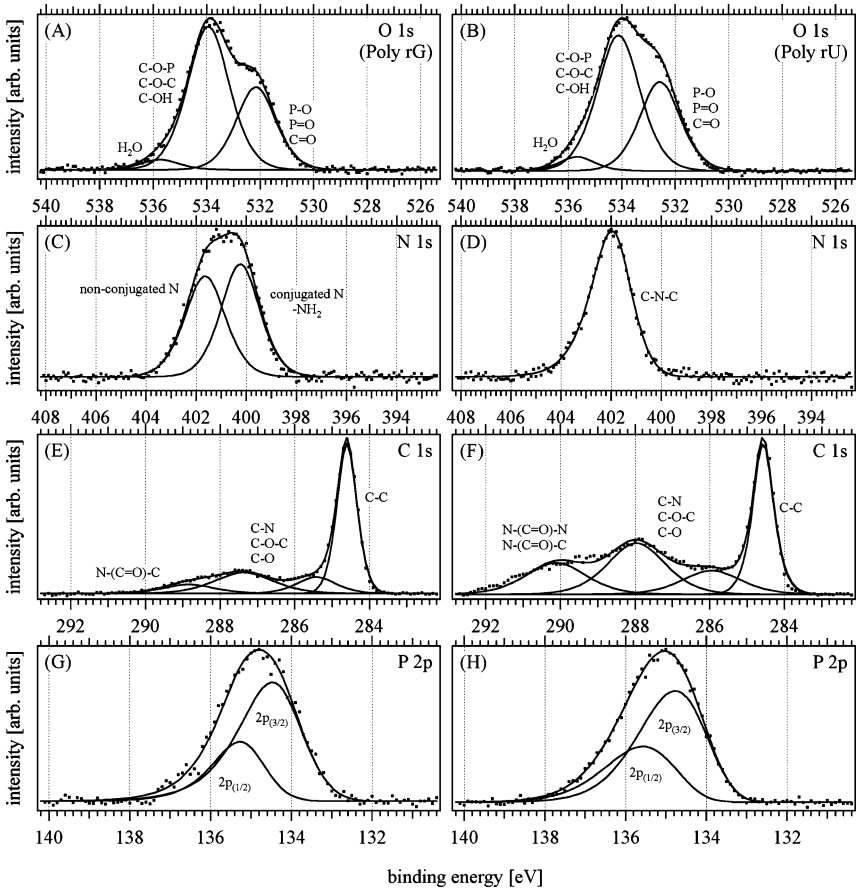

Figure 3. O 1s, N 1s, C 1s, and P 2p spectra (dots) measured with monochromatized XPS on poly rG (A, C, E, G) and poly rU (B, D, F, H) thin films deposited on HOPG. The full lines represent the Gaussian−Lorentzian peaks that were fit to each emission region.

B. Electronic Structure. Determination of the electronic structure of the interface between HOPG and each nucleotide was accomplished by evaluating the UP spectra. As is obvious from the UP spectra shown in Figure 2, the secondary edge strongly shifts to higher binding energy due to sample charge-up during the UPS measurement, similar to what was seen in the measurements on poly rA and poly rC. As in these experiments, the high binding energy cutoff is immediately affected after the first deposition steps for each nucleotide, while the HOMO maxima appear to remain at about the same binding energy during all of the deposition steps. This can be explained by the different mechanisms affecting the high and low binding energy sides of emission features if inhomogeneous charging occurs (as can be assumed to be the case in these experiments because the overlayers are being built up slowly). This is shown in Figure 4, where the emissions of a surface with a partially charged area are schematically compared to those of a completely uncharged surface. After partial charging occurs, primary peaks represent a composite of emissions from uncharged (shown in gray) and, shifted to higher binding energy, from charged (shown in black) areas. The results are a shift of the peak onset on the *high* binding energy side equal to the total electrical potential caused by the charges, a reduced shift of the peak maximum (caused by the superposition with the emissions related to the uncharged areas), while the peak onset position on the *low* binding energy side is more or less unaffected (the onset only gets flatter as the cumulative peak is widening, but remains at the same position). Because the secondary cutoff practically represents the *high* binding energy cutoff of the entire photoemission spectrum, charging artifacts

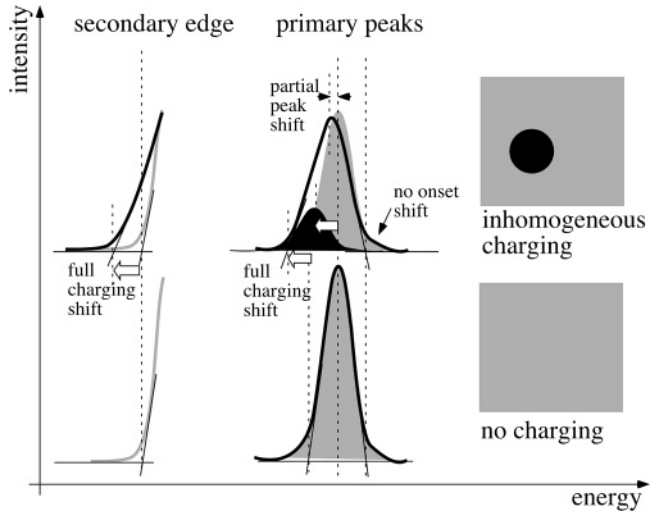

Figure 4. Effects of partial surface charging on primary photoemission peaks and the secondary edge feature. Areas of the surface which are charged result in emissions (shown in black) shifted to higher binding energy. In the case of primary peaks, this causes a widening of the peak. The low binding energy onset of the peak remains at the same location, while the peak maximum incurs a partial shift and the high binding energy cutoff exhibits the full charging shift. The secondary edge behaves like the high binding energy cutoff, i.e., shows the full charging shift. Therefore, it is possible to still evaluate the low binding energy onset of a peak in the case of partial charging, while the secondary edge can only be evaluated unambiguously in the absence of charging.

TABLE 1: Values Used to Calculate Absolute Peak Intensities for Stoichiometric Evaluation

					poly rG		poly rU	
	cross section (CS)	mean free path (MFP) [Å]	kinetic energy (E_{kin}), [eV]	transmission factor (TF)	peak area (A)	normalized absolute intensity ($I_{absolute}$)[a]	peak area (A)	normalized absolute intensity ($I_{absolute}$)[a]
N 1s	1.8	28	1086	0.030	1009	3.54	669	1.44
O 1s	2.93	26	956	0.032	2650	5.76	4861	6.48
P 2p	1.18	34	1351	0.027	205	1.0	333	1.0
C 1s (C−N, C−O)[b]	1.0	31	1202	0.029	1705	10.04	2907	10.51

[a] Absolute intensities are calculated with respect to the P 2p peak area. [b] C 1s peak areas and intensities only include C−N, N−C−N, C−O, and N−(C═O)−N emissions because HOPG emissions superimpose C−C line.

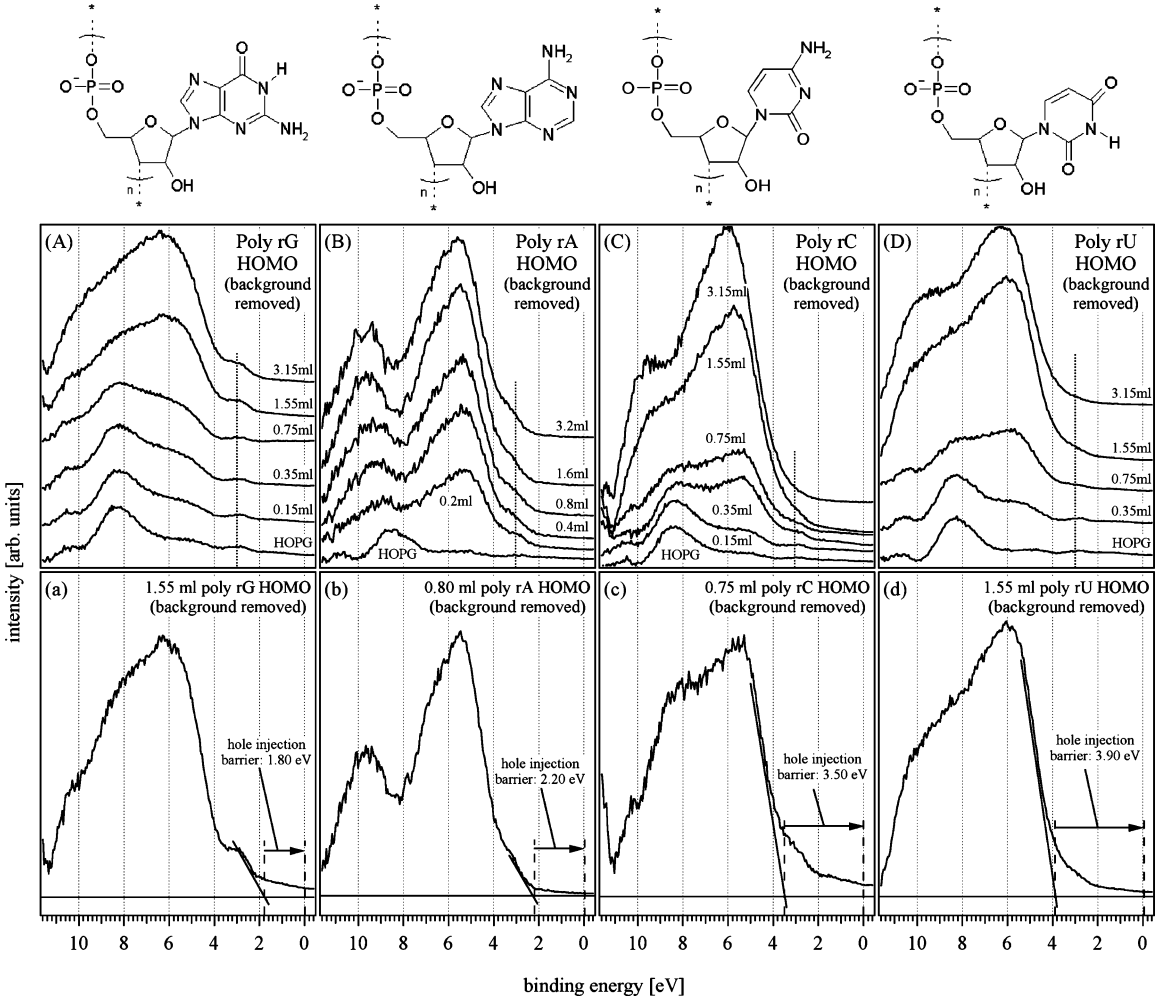

Figure 5. Determination of the hole injection barriers at the poly rG/HOPG (A, a), poly rA/HOPG (B, b), poly rC/HOPG (C, c), and poly rU/HOPG (D,d) interfaces. The top row shows the UPS HOMO region of each of the deposition sequences with background removed. The bottom row shows the selected spectrum for the HOMO cutoff determination including line fitted to the spectral onset. The purines poly rG and poly rA have a distinctive feature at the low binding energy onset, which is not evident in the pyrimidine spectra. This results in significant differences between the ionization energies and hole injection barriers relative to the HOPG Fermi level.

occurring on a small percentage of the surface will strongly affect the cutoff, while primary peaks will exhibit a comparably smaller shift. Peak onset positions on the low binding energy side should in principle not be affected at all.

The top graphs of Figure 5 show the spectral region of the UP spectra corresponding to the HOMO emissions with removed background for all four nucleotides, including those of poly rA (from ref 14) and poly rC (from ref 15). The background removal was performed by fitting the integral of the spectrum to the regions around the HOMO features (see ref 14 for details).

A distinct difference between the pyrimidine nucleotides and purine nucleotides becomes obvious when comparing the evolution of each of the HOMO emissions. The bottom spectra of all four series correspond to vacuum-cleaved HOPG. Three HOPG valence bands related emissions regions are seen at approximately 8, 5, and 3 eV (denoted by dotted lines). The emissions at 8 and 5 eV are attenuated on all four samples as the nucleotide layer increases in thickness. However, the emission feature at 3 eV is only attenuated in the pyrimidine experiments, while on poly rG and poly rA, this feature appears to increase in signal as the layer thickness increases. This suggests that the purines feature a HOMO related emission at this binding energy while the pyrimidines do not. Hence, in the case of the pyrimidines, the HOMO onset appears to be located on the main

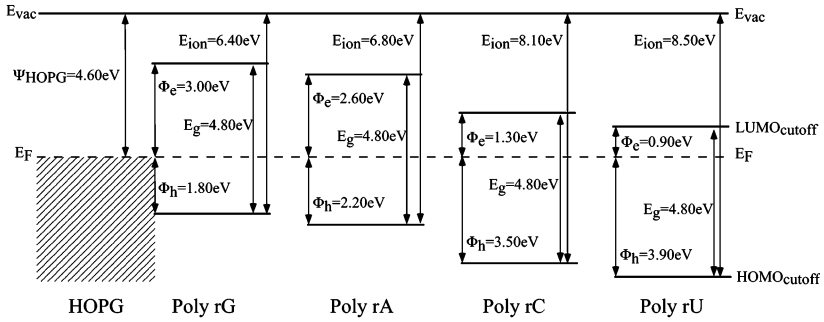

Figure 6. Schematic depictions of the orbital line-ups for the four investigated ribonucleic acid homopolymer interfaces to HOPG. Each interface exhibits significant charge barriers in both directions, suggesting poor charge transfer. A significant difference between purine and pyrimidine ionization energies (E_{ion}) and hole injection barriers (Φ_h) was found. The electron injection barriers (Φ_e) were estimated using a HOMO−LUMO gap of 4.8 eV, as determined by absorption measurements of nucleotides in solution.

emission feature, while, in the case of the purines, the HOMO onset is located on the cutoff of the small feature at around 3 eV.

This difference in the HOMO structures causes a significant difference between the charge injection barriers and ionization energies observed on these materials. Panels (a− d) show the HOMO cutoff determination in detail. The 1.55 mL spectra were chosen for HOMO onset evaluation of the poly rG and poly rU onsets because charging effects are still largely absent, while the substrate emissions are sufficiently attenuated to allow a confident cutoff evaluation. Furthermore, these spectra correspond to polynucleotide layers of similar thickness (12−15 Å), similar to the spectra used for the evaluations performed earlier on poly rA and poly rC. The HOMO cutoff binding energies for each of the nucleotides was estimated by fitting lines to the low binding energy side of their HOMO emissions and calculating the intersect with the binding energy axis. The fitted lines are shown schematically drawn into the onsets, shifted by 0.1 eV to account for the analyzer broadening of the spectra. Determination of the intersects of the fitted lines with the *x*-axis yielded binding energies of 1.8 eV for poly rG, 2.2 eV for poly rA, 3.5 eV for poly rC, and 3.9 eV for poly rU. Because the binding energies are referenced to the Fermi level of the HOPG substrate at 0 eV, these values correspond directly to the hole injection barriers (Φ_h) between HOPG Fermi level and nucleotide HOMOs.

Because of the purely charging related origin of the secondary cutoff shifts in the UP spectra, it can be concluded that, in agreement with the earlier results on poly rA and poly rC, interface dipoles are absent at the HOPG/poly rU and HOPG/poly rG interfaces. The reason for this behavior is the high chemical inertness of HOPG and the formation of only weak van der Waals bonds at the interface, which entail only insignificant local charge transfer across the interface. This has also been observed on other experiments on HOPG/organic molecule interfaces,[26,27] supporting this conclusion.

These considerations allow depiction of the orbital line-up at the interface to HOPG as well as the determination of the ionization energies of the nucleotides. Figure 6 shows these results summarized for all four nucleotides. The results for poly rA (E_{ion} = 6.8 eV, this value is misstated in ref 14 as "7.8 eV" due to a miscalculation) and poly rC (E_{ion} = 8.1 eV) were taken from refs 14 and 15. The ionization energies given in the figure for poly rG (E_{ion} = 6.40 eV) and poly rU (E_{ion} = 8.50 eV) were determined in the same way by adding the work function value measured on the HOPG surface and the respective HOMO cutoff positions. This can be done due to the absence of interface dipoles.

The corresponding LUMO positions (i.e., the electron injection barriers (Φ_e)) were estimated by assuming a HOMO−LUMO gap of 4.8 eV, which was determined on nucleotides in solution by UV absorption[28] (to the knowledge of the authors, there are no UV−vis measurements on nucleotide thin films published to date). This yielded electron injection barriers (Φ_e) between the Fermi level of HOPG and nucleotide LUMO of 3.0 eV for poly rG and 0.9 eV for poly rU. The values for poly rA (2.60 eV) and poly rC (1.30 eV) were obtained in an identical way (from refs 14 and 15). It should be kept in mind that these values are only crude estimates because measurements in solution consider solvated single molecules, while thin films in vacuum represent a solid-state configuration of the molecules. Furthermore, optical gap measurements include exciton features, which may be several tenths of an electronvolt in organic molecules.[29] With regard to measurement errors, the stated ionization energy and injection barrier values probably contain errors of approximately ±0.2 eV due to the broad shape of the HOMO peaks. It is interesting to note that all four orbital line-ups have fairly large charge injection barriers in both directions, predicting poor charge transfer across all of the interfaces. This is supported by the early onset of charging artifacts in the UP spectra series, which suggests a reluctant replenishment of the emitted photoelectrons caused by an impaired charge transfer from the HOPG substrates to the homopolymer overlayers. The large differences between the charge injection barriers related to each of the nucleotide homopolymers suggest that it is of crucial importance for the charge injection in conductivity measurements where the contact is made on a nucleotide strand. In other words, depending on the contacted nucleotide species, large differences in the injected current can be expected due to the exponential dependency of the injection current on the barrier height. This may partially explain the large spread of results in conductivitiy measurements on single-strand DNA.

The nucleotide type specific ionization energy differences imply that the energy required for ionization is determined by the nitrogenous base rather than the ribose−phosphate backbone, which is supported by gas-phase PES measurements and theoretical calculations by LeBreton et al.: comparison of the UP spectra of standard compounds related to uracil, ribose, and uridine show that uracil primarily accounts for the HOMO emissions of uridine.[4] Furthermore, ab initio calculations on adenosine and adenine confirm that ribose and phosphate related ionization energies are larger than that of adenine.[30]

When comparing the ionization energy values with results on nucleobases, mononucleosides, and mononucleotides, the values agree qualitatively with experimental and calculated data in that the ionization energies follow $E_{ion}(G) < E_{ion}(A) < E_{ion}(C)$

TABLE 2: Ionization Energies of Nucleobases, Nucleosides, Nucleotides, and Nucleotide Homopolymer Thin Films

	method	guanine	adenine	cytosine	uracil	ref
Poly rX films on HOPG	PES	6.4	6.8	8.1	8.5	this paper
Bases						
Orlov et al.	ion current	7.77	8.26	8.68	9.32	5
Yu et al.	gas-phase UPS	8.23	8.49	8.95	9.54	4
Close	calcd	8.13	8.49	8.79	9.54	1
Dolgounitcheva et al.	calcd	8.38		8.79−8.83	9.54	2, 3
Nucleosides						
Yu et al.	gas-phase UPS/calcd	8.0	8.4	8.6	9.0	4
Nucleotides						
Yang et al.	gas-phase UPS/electrospray	5.05	6.05	5.80		6
Dolgounitcheva et al.	calcd				7.25	2
Oligonucleotides						
Kim et al. (hexamer stacks of bases)	calcd	6.36−6.98				31
Yang et al. (trinucleotides)	gas-phase UPS/electrospray	5.27	5.62	5.78		6

$< E_{ion}$(U). Table 2 shows the here determined ionization energies for nucleotide polymers in comparison with the other findings. Photoionization threshold measurements by Orlov et al. yielded the first published ionization energies of 7.77 eV for guanine, 8.26 eV for adenine, 8.68 eV for cytosine, and 9.32 eV for uracil.[5] Subsequently, measured gas-phase UPS data by Yu et al. resulted in somewhat higher values of 8.23 eV (G), 8.49 eV (A), 8.95 eV (C), and 9.54 eV (U). Theoretical investigations by Close et al.[1] and Dolgounitcheva et al.[2] closely confirmed these values. Yu et al. used the above nucleobase ionization energies to estimate nucleoside ionization energies yielding 8.0 eV for guanosine, 8.4 eV for adenosine, 8.6 eV for cytidine, and 9.0 eV for uridine.[4] These values are smaller than the nucleobase energies, which is likely a result of the enhanced screening of the resulting hole due to the larger molecule size.

This effect progresses in nucleotide ionization energies, which were found to be even smaller. Calculations of the guanine ionization energy in various heteropolymer oligonucleotide environments yielded values of 6.36−6.98 eV.[31] These values agree well with the obtained ionization energy of poly rG of 6.4 eV. Experimental investigation of negative mono- and trinucleotide ions injected into vacuum using an electrospray injection mass spectrometer, combined with an electron energy analysis capability, yielded even lower ionization energies (see Table 2).[6] It is interesting to compare the photoemission spectra shown in ref 6 with the HOMO spectra shown in Figure 4. In the case of the mononucleotides, ref 6 shows that guanosine exhibits a small peak at lower binding energy in addition to the main HOMO emission seen on all nucleotide species. This corresponds well to the guanosine homopolymer HOMO spectra shown in Figure 5A. However, this was not seen in in ref 6 for the case of single adenosine molecules, which is in contrast to the measurements on poly rA, where a less separated, but clearly identifiable low binding energy emission was detected (compare Figure 5B). In ref 6 it is stated, based on theoretical calculations, that only guanosine has the HOMO located on the base, while the HOMO of the other nucleotides is located on the phosphate group. This apparently changes once longer nucleotide chains are formed. Additional measurements on trinucleotides in ref 6 indicated that, in the case of adenosine, a small emission tail arose, reducing the ionization energy by 0.43 eV compared to monoadenosine. This trinucleotide spectrum agrees well with the poly rA spectra shown in Figure 5. Comparing the absolute ionization energy values between the data shown here and ref 6, it occurs that the values in ref 6 are smaller than the values presented here. This might be the result of the negative charge on the investigated gas-phase ions, which probably lowers the ionization energy considerably. In contrast, while the nucleotide homopolymer molecules were also injected using electrospray, their negative charges were likely neutralized or screened upon deposition on the conductive HOPG substrate, resulting in larger ionization energies.

Conclusion

Polyguanidine (poly rG) and polyuridine (poly rU) homopolymers were deposited in several steps on highly ordered pyrolytic graphite (HOPG) in vacuum using electrospray injection. Photoemission spectroscopy (PES) evaluation using X-ray and ultraviolet radiation (XPS, UPS) of the substrate before and after each deposition step allowed the determination of the ionization energies of poly rG and poly rU as well as the electronic structure of each oligonucleotide/HOPG interface. Stoichiometry evaluation yielded similar results to previously performed XPS analyses of ex situ prepared nucleotide thin films. Large and strongly varying charge injection barriers were found on each of the investigated interfaces, and no significant interface dipoles were detected. Ionization energies of poly rU and poly rG were determined to be 8.5 and 6.4 eV, respectively. These values completed the series of measurements on the four ribonucleotide homopolymers, establishing the relative magnitudes of the ionization energies for the nucleotide as E_{ion}(G) < E_{ion}(A) < E_{ion}(C) < E_{ion}(U).

Acknowledgment. Financial support by the National Science Foundation (grants DMR 0510000 and DMR 0205577) is gratefully acknowledged. J.M. acknowledges partial funding through an Engineering Undergraduate Research Fellowship provided by the USF College of Engineering Research Experience for Undergraduates program (http://www.eng.usf.edu/~schlaf/REU/).

References and Notes

(1) Close, D. M. *J. Phys. Chem. A* **2004**, *108*., 10376−10379.

(2) Dolgounitcheva, O.; Zakrzewski, V. G.; Ortiz, J. V. *Int. J. Quantum Chem.* **2002**, *90*, 1547−1554.

(3) Dolgounitcheva, O.; Zakrzewski, V. G.; Ortiz, J. V. *J. Phys. Chem. A* **2003**, *107*., 822−828.

(4) Yu, C.; Odonnell, T. J.; Lebreton, P. R. *J. Phys. Chem.* **1981**, *85*, 3851−3855.

(5) Orlov, V. M.; Smirnov, A. N.; Varshavsky, Y. M. *Tetrahedron Lett.* **1976**, *48*, 4377−4378.

(6) Yang, X.; Wang, X. B.; Vorpagel, E. R.; Wang, L. S. *Proc. Natl Acad. Sci. U.S.A.* **2004**, *101*, 17588−17592.

(7) Fink, H. W.; Schonenberger, C. *Nature* **1999**, *398*, 407−410.

(8) Porath, D.; Bezryadin, A.; de Vries, S.; Dekker: C. *Nature* **2000**, *403*, 635−638.

(9) Cuniberti, G.; Craco, L.; Porath, D.; Dekker: C. *Phys. Rev. B* **2002**, *65*, 241314(R).

(10) Storm, A. J.; van Noort, J.; de Vries, S.; Dekker: C. *Appl. Phys. Lett.* **2001**, *79*, 3881−3883.

(11) Cai, L. T.; Tabata, H.; Kawai, T. *Appl. Phys. Lett.* **2000**, *77*, 3105−3106.

(12) Seeman, N. C.; Lukeman, P. S. *Rep Prog Phys* **2005**, *68*, 237−270.

(13) Mucic, R. C.; Storhoff, J. J.; Mirkin, C. A.; Letsinger, R. L. *J. Am. Chem. Soc.* **1998**, *120*, 12674−12675.

(14) Dam, N.; Doran, B. V.; Braunagel, J. C.; Schlaf, R. *J. Phys. Chem.* **2005**, *109*, 748−756.

(15) Magulick, J.; Beerbom, M. M.; Lagel, B.; Schlaf, R. *J. Phys. Chem.* **2006**, *110*, 2692−2699.

(16) Waldrop, J. R.; Grant, R. W. *Phys. Rev. Lett.* **1979**, *43*, 1686−1689.

(17) Dam, N.; Beerbom, M. M.; Braunagel, J. C.; Schlaf, R. *J. Appl. Phys.* **2005**, *97*, 024909.

(18) Seah, M. P. *Surf. Interface Anal.* **1989**, *14*, 488.

(19) Kohlscheen, J.; Emirov, Y. N.; Beerbom, M. M.; Wolan, J. T.; Saddow, S. E.; Chung, G.; MacMillan, M. F.; Schlaf, R. *J. Appl. Phys.* **2003**, *94*, 3931−3938.

(20) Kojima, I.; Kurahashi, M. *J. Electron. Spectrosc. Relat. Phenom.* **1987**, *42*, 177.

(21) May, C. J.; Canavan, H. E.; Castner, D. G. *Anal. Chem.* **2004**, *76*, 1114−1122.

(22) Moulder, J. F.; Stickle, W. F.; Sobol, P. E.; Bomben, K. D. *Handbook of X-ray Photoelectron Spectroscopy*; Physical Electronics, Inc.: Eden Prairie, MN, 1995.

(23) Briggs, D.; Beamson, G. *Anal. Chem.* **1993**, *65*, 1517−1523.

(24) Saprigin, A. V.; Thomas, C. W.; Dulcey, C. S.; Patterson, C. H.; Spector, M. S. *Surf. Interface Anal.* **2005**, *37*, 24−32.

(25) Jones, T. S.; Ashton, M. R.; Richardson, N. V.; Mack, R. G.; Unertl, W. N. *J. Vac. Sci. Technol., A* **1990**, *8*, 2370−2375.

(26) Schlaf, R.; Parkinson, B. A.; Lee, P. A.; Nebesny, K. W.; Armstrong, N. R. *Surf. Sci.* **1999**, *420*, L122-L129.

(27) Schroeder, P. G.; France, C. B.; Parkinson, B. A.; Schlaf, R. *J. Appl. Phys.* **2002**, *91*, 9095−9107.

(28) Petrovykh, D. Y.; Kimura-Suda, H.; Tarlov, M. J.; Whitman, L. J. *Langmuir* **2004**, *20*, 429−440.

(29) Pope, M.; Swenberg, C. E. *Electronic Processes in Organic Crystals and Polymers*; Oxford University Press: Oxford, 1999.

(30) Kim, N. S.; Jiang, Q.; Lebreton, P. R. *Int. J. Quantum Chem.* **1996**, *60*, 11−19.

(31) Kim, N. S.; Qiqing, Z.; LeBreton, P. R. *J. Am. Chem. Soc.* **1999**, *121*, 11516−11530.